High Density Polyethylene (HDPE) and Polypropylene (PP) Polyblend: An Experimental Approach

Chapter · September 2019

DOI: 10.9734/bpi/namse/v1

5 authors, including:

Harekrushna Sutar
Indira Gandhi Institute of Technology
49 PUBLICATIONS **403** CITATIONS
SEE PROFILE

Rabiranjan Murmu
Indira Gandhi Institute of Technology
28 PUBLICATIONS **136** CITATIONS
SEE PROFILE

Subash Chandra Mishra
National Institute of Technology Rourkela
189 PUBLICATIONS **1,971** CITATIONS
SEE PROFILE

Chapter 4
Print ISBN: 978-93-89246-08-7, eBook ISBN: 978-93-89246-26-1

High Density Polyethylene (HDPE) and Polypropylene (PP) Polyblend: An Experimental Approach

Harekrushna Sutar[1*], Rabiranjan Murmu[1], Chiranjit Dutta[1], Mutlu Ozcan[2] and Subash Chandra Mishra[3]

DOI: 10.9734/bpi/namse/v1

ABSTRACT

The present research focuses to evaluate a complete outlook of virgin high density polyethylene (HDPE) and polypropylene (PP) polyblends. Virgin PP of 10, 20, 30, 40 and 50 weight % is compounded with virgin HDPE. Tensile, Flexural and impact test specimens of virgin HDPE, Virgin PP and HDPE-PP composites are prepared via twin screw extruder and injection moulding methods as per ASTM D638-02a (Type-I), ASTM D790 and ASTM D256-A standards respectively. The mechanical properties like tensile strength, flexural strength, Izod impact strength are examined. Polymer sheets are fabricated using a two roll milling machine and compression moulding; and its electrical properties like dielectric strength, surface resistivity, volume resistivity are examined according to ASTM-D 257 standard. The study also includes effect of strain rate on tensile properties of the prepared composite at a cross head speed of 30, 40, 50, 60 and 70 mm/min. Design of experiment is conducted to find parameters dominating the tensile strength. All experiments are carried out at room temperature of 23℃ and absolute humidity of 54%. Scanning electron microscopy (SEM), Atomic force microscopy (AFM) and polarised light microscopy (PLM) are used to observe the surface and crystal morphology. X-ray diffraction (XRD), Fourier transform infrared spectroscopy (FTIR) tests verify the non compatibility of both polymers. Differential scanning calorimetry (DSC) and thermogravimetric analysis (TGA) techniques are used to study the thermal behaviour of composites. The results manifest dielectric strength and volume resistivity decreases with addition of PP to HDPE; whereas surface resistivity increases. Co-occurring spherulites are seen for polyblends; indicating the composite to be a physical blend of continuous and dispersed phases, but on the other hand PP improves the tensile and flexural properties of HDPE.

Keywords: High density poly ethylene (HDPE); Polypropylene (PP); polyblends; mechanical; thermal; crystallization; electrical properties; strain rate.

1. INTRODUCTION

Polymer composite is material of research in modern days. Thermoplastic polymers are of great interest due to their technical and commercial importance [1]. In general two or more polymers are melt blended to form a product as polyblends [2-5]. The component percentages are the primary factor influencing their physical properties [6]. The manufacturing technique and operating conditions are second governing factor.

Among the thermoplastic polymers; PP possess good mechanical strength. In addition it has high chemical resistance, low cost and easy to manufacture. PP has wide application in automobile spare parts and as well as container [7]. HDPE is known for its large strength to density ratio due to its little branching .HDPE unlike PP cannot withstand normally required autoclaving conditions [8-13].

[1]Department of Chemical Engineering, Indira Gandhi Institute of Technology, Sarang, India.
[2]Center for Dental and Oral Medicine Clinic for Fixed and Removable Prosthodontics and Dental Materials Science, University of Zurich, Switzerland.
[3]Department of Metallurgical and Materials Engineering, National Institute of Technology, Rourkela, India.
**Corresponding author: E-mail: h.k.sutar@gmail.com;*

Jia-Horny Lin et al. has reinforced HDPE to PP matrix and verified the non-compatibility of both polymers, but improves the impact strength of PP [14]. Souza et al. found the effect of processing temperature and content of HDPE on interfacial tension of the PP/HDPE polyblend [15].

Past studies show the compatibility of PP/HDPE polyblends depends on factors like processing temperature, polymer structure and blending ratios [15-17]. Polymers with similar physical properties form polyblends with greater mechanical strength [18-20]. The mechanical properties of the PP/HDPE polyblend decreases with increase in dissimilarity of melt flow index (MFI) [21]. During last decades polymeric containing materials attracted the attention of scientists for wide spread applications such as solar energy conversion, coatings, adhesives, lithography, light emitting diodes, sensors, laser development and many applications [22,23]. Thermoplastics are used in various electrical applications like wire and cable as insulation and jacketing materials due to their unique combination of properties such as low temperature flexibility, excellent insulating characteristics and resistance to moisture absorption [24]. Electrical properties of various polymer blends have been investigated by different researcher [25-31]. In general polymer blends are prepared by physical mixing of two or more polymers to obtain a new material with improved properties compared to the parent one. This is the most convenient method of obtaining a material rather than synthesizing a new polymer [32,33]. The electrical conductivity studies are aimed at understanding the origin of the charge carrying species and the way in which they move through the bulk of the material. Polymers with controlled conductivity and thermal sensitivity are much desirable in various applications [34-36]. Knowledge of electrical properties of polymer blends is helpful in material study and characterization for device fabrication.

To develop a new electrical insulating material with good performance, it is important to do researches focusing on the effect of morphology on electrical properties. Polypropylene possesses good insulation performance because of its high crystallinity. However, since spherulite boundaries become weak points, the dielectric strength of polypropylene is not so much higher than high density polyethylene [37,38]. It is reported that by blending polyethylene with polypropylene, the dielectric strength can be increased because the spherulite boundaries are reinforced [39-41]. The mechanism of increase in dielectric strength by polymer blending is still not so clear.

History reveals, the composites are mainly used for savings in secondary structures. The fibre-reinforced polymer (FRP) materials find increasing applications as load bearing structures. But in the other hand, development of polymer materials for high technology engineering applications is in demand [42-44]. It is always a matter of concern, to evaluate the mechanical properties of polymer composites at high rates of strain. Premature failure at high loading rates alarms to design structures with high strength. The progress in research to find the mechanical strength of thermoplastic polymer blends are still lacks. With respect to above argument, a polymer blend of HDPE-PP has been developed to understand the strain rate effects on particularly to tensile properties.

A detailed review of the strain rate dependence of mechanical properties of polymer composites has been outlined by Jacob et al. [45]. The study of different properties of polymer blends is a new approach [46]. These polymeric materials must perform at the imposed conditions. Blend of HDPE-PP has been prepared [47-49] and its mechanical, thermal, crystallization and electrical properties has been studied. An experimental approach using universal testing machine (UTM) was employed to study the effect of low strain rate loading on HDPE/saw dust composites [50]. In fibre reinforced polymer composites, the increment of filler may increase its tensile strength [51]. In general, the filler is incapable to endure the stress transmission efficiently and resulting low compression strength [52,53]. In a similar manner, Bia et al. [54] studied the tensile properties of rigid glass bead/HDPE composites at a strain rate of 3×10^{-5} - 8×10^{-3} s^{-1} and observed tensile modulus and strength increases with loading rate. Over the last two decades, the global production of synthetic polymers increasing. Polymers have low weight, durability and cheap relative to other materials [55-57]. So in the present work an attempt has been made to find out an alternative use of HDPE-PP polyblend by accessing the different physical and chemical properties. Additionally the design of experiments (DOE) is carried out to discover the influencing factor on tensile strength at break point.

2. EXPERIMENTAL

2.1 Collection of Polymers

PP (M110 Grade, homopolymer) produced by the sphericol technology and HDPE (M5818 Grade, injection moulded type) produced by Mitsui Slurry CX technology are purchased from Haldia petrochemical limited, haldia, India. Different physical properties of the polymers are reported in Table 1.

Table 1. Physical properties of polymers

Polymer type	Melt flow index (g/10 min)	Density(g/cc)
HDPE	19 (2.16 kg,190℃)	0.956
PP	11 (2.16 kg, 230℃)	0.900

2.2 Preparation of Tensile, Flexural and Impact Test Specimen

Polymers in the form of pellets are collected. The pellets are dried in a hot air oven at 60℃ for 8 hrs to remove moisture content followed by mixing of 10, 20, 30, 40 and 50 wt. % of PP to HDPE. Then they are converted into polymer blend pellets using a twin screw extruder (ZV20, Specific Engineering and Auto Mates, Vadodara, India) at feeder speed of 51 rpm and main rotor at 54 rpm. The screws are of 21 mm diameter and co-rotating type, containing three thermal barrels at 190, 200 and 210℃ respectively. The melt and die temperatures are 224 and 200℃.

The obtain pellets are dried at 60℃ for 8 hrs and moulded to test samples using an automatic injection moulding machine (Endura-90, Electonica plastic machines limited, Kolkata, India) with screw diameter of 35 mm at 177 rpm. The temperature of the nozzle is 200℃ and that of the three barrels are 190, 200 and 210℃ respectively.

Tensile specimens are prepared according to ASTM D638-02a type-I; with gage length 50 mm, width 13 mm and thickness 3 mm. Flexural sample of size 127 mm × 12.7 mm × 3.2 mm are prepared as per ASTM D790 standards. Impact test specimens are prepared by cutting the flexural samples to a size of 63.5 mm × 12.7 mm × 3.2 mm with a V-notch of 45° and 0.25 mm depth as per as per ASTM D256-A standard. Fig. 1 shows the snapshots of the test samples.

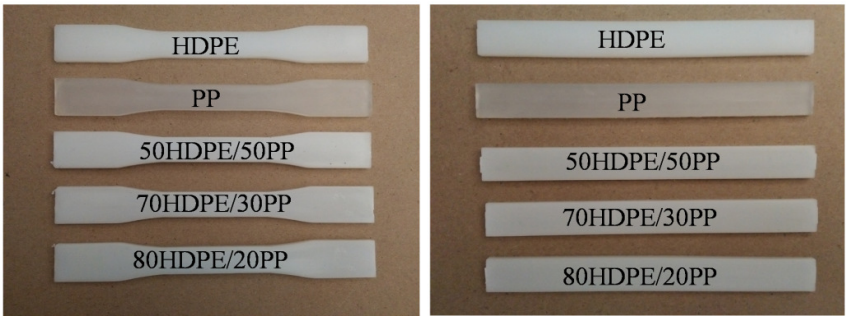

(a) (b)

Fig. 1. Prepared test specimens (a) Tensile (b) Flexural

2.3 Preparation of Polymer Sheets

In the similar manner collected polymer pellets are dried in a hot air oven at 60℃ for 8 hours to remove moisture content followed by mixing of 20, 30 and 50 weight % of PP to HDPE. They are converted into polymer raw sheets using a two roll milling machine having front roll at a speed of 42 rpm and rear roll at a speed of 37 rpm at an operating temperature of 300℃. The rollers are of 155

mm diameter and 360 mm length. The raw sheets are chopped and finally converted to circular disc shaped sheets having Φ of 110 mm (for surface and volume resistivity) and 50 mm (for dielectric strength) with 3 mm thickness using a laboratory compression press (Identification no: CIPET/PTC/119, make: CIPET, Ahmedabad) as per ASTM-D 1894 standard at 300℃ and 15 tons load. The circular disc shaped polymer sheets used in the experiment are shown in Fig. 2.

Fig. 2. Polymer sheets incorporated for electrical property study

2.4 Mechanical Properties

Both tensile and flexural strengths of HDPE/PP polyblends are tested using an universal testing machine (UTM3382, Instron, UK) as per ASTM D638-02a and ASTM D790 standards respectively. Mechanical properties are studied for the composites along with virgin polymers and results are compared. Tests are conducted at cross head speed of 50 mm/min (ASTM standard). Flexural sample of size 127 mm × 12.7 mm × 3.2 mm are tested at speed of 1.365 mm/min with support span spacing of 51.2 mm (span = 16 times of thickness) at an extension up to 5%. The speed of the test and flexural strengths are calculated according to equation 1 and 2 respectively.

$$Speed = \frac{ZL^2}{6d} \tag{1}$$

$$\sigma_{F_{max}} = \frac{3PL}{2bd^2} \tag{2}$$

Where, Z is Rate of straining at 0.01 mm/mm/min, L is span length (mm) and d is sample thickness (mm), $\sigma_{F_{max}}$ is flexural strength (MPa), P is load (N), L is span length (mm) and b is sample width (mm).

Impact tests are conducted using a Izod and Charpy impactometer (IT 504 Plastic impact, Tinius Olsen, USA) with a V-notch cutter as per ASTM D256-A standard , possessing a pendulum energy of 13.70 J. Impact test specimens are prepared by cutting the flexural samples to a size of 63.5 mm × 12.7 mm × 3.2 mm with a V-notch of 45° and 0.25 mm depth.

Mechanical property study also includes the findings like, the strain rate effect on tensile strength. Tests are conducted at cross head speed of 30, 40, 50, 60 and 70 mm/min for each composite type.

Stress and strain at yield and break points are estimated in the experiment and reported in result and discussion section. Each data corresponds to the mean value for three independent observations.

2.5 Microscopy Test

Our investigation has used SEM (JEOL; JSM-6480 LV, USA), Field emission SEM (Nova Nano SEM-450, USA) and PLM (Leica, DM750P, Germany). Morphology of samples is captured before and after fracture of impact test. Energy dispersive spectroscopy (EDS) analysis and carbon mapping test are conducted using FESEM at an operation voltage of 10 KV. Samples are gold coated before each test. PLM is used to observe the spherulite behaviour of the polyblends. A tiny sample is placed on a glass slide and melted at 200℃ (using the hot stage) followed by sandwiching the sample by placing a micro glass slide over it to form a thin film. The sample is cooled at rate of 5℃/min (using cold stage) and spherulite morphologies are captured at 130 and 125℃ at magnification×10.

AFM (Park XE 100, South Korea) is used to observe the topography of prepared tensile specimens. In order to see the distribution of polymer molecules in the blend and root mean square (rms) roughness (R_q) in nanometre scale; an AFM at non contact mode and room temperature is implemented. Images were scanned by using a cantilever of tip radius 10 nm (NCHR mode), a nominal constant spring of 0.05 N/m and a scanning rate of 0.9 Hz. The scans were made on 1000 nm × 1000 nm scale (except for 60HDPE/40PP, held at 750 nm × 750 nm) and repeated five different times on five different area of the polymer surface (tensile specimen) at a resolution of 256 × 256 pixels (except for 60HDPE/40PP, held at 192 × 192 pixels), set point of 10 nm, amplitude of 20.85 nm. The rms roughness is determined [58] by following equation,

$$\mathrm{rms} = \frac{\sqrt{(Z_i - Z_{av})^2}}{N} \tag{3}$$

Where, Z_i is the height at a particular point on an image (nm), Z_{av} is the mean height of all pixels in the image (nm) and N is the total number of pixels in the image. The maximum range is the height difference between the lowest and highest pixels in the image.

2.6 XRD, FTIR

In order to analyse any new phase formations after blending the polymers and to understand the chemical structure of the polyblends; the XRD (Philips, PW1720, USA) and FTIR (Perkin-Emler Spectrum 100, USA) techniques are utilised. X-ray scanning is done within a diffraction angle (2θ) range of 10-90° with Cu Kα radiation at 40 KV and 30 mA. The rate of scanning is 10°/min and at λ = 0.154 nm. The IR Spectroscopy is observed between the waveband of 450 to 4000 cm^{-1}.

2.7 Dsc and Tga Analyses

The polyblends thermal behaviour is analysed using a DSC (Perkin-Elmer DSC 7, MA, USA) and TGA (Perkin-Elmer TGA, MA, USA) analysers. The DSC tests are performed under nitrogen flow rate of 50 ml/min. Polymer samples of around 10 mg are scanned at a heating rate of 10℃/min from ambient temperature to 200℃. The samples undergo three thermal cycles. Heating, cooling and reheating under the same condition to follow an identical thermal history for all polymer blends.

The degree of crystallinity (X_C) of the polyblends is evaluated by equation-4

$$X_C(\%) = \frac{\Delta H_f}{\emptyset\, \Delta H_f^0} \times 100 \tag{4}$$

Where, ΔH_f = Melting enthalpy of HDPE or PP in the blend, ΔH_f^0 = Enthalpy corresponding to melting of 100% crystalline HDPE or PP and Ø = weight fraction of HDPE or PP in the blend. In TGA test, polymer samples with masses of approximately 10 mg are heated from atmospheric temperature to

600℃, at heating rate of 10℃/min and nitrogen flow rate of 50 ml/min, to observe their degradation behaviour. Data corresponding to ΔH_f^0 are referred from Roger L. Blaine [59].

2.8 Taguchi Optimization

Design of experiment (DOE) is one of the powerful statistical techniques to study the influence of the controlling factor on output. All designed experiments require a certain number of combinations of factors and levels be tested in order to observe the results of those test combination. In our project, Taguchi optimization method is employed to find out the optimum operating parameters influencing the tensile properties using MINITAB-16 software. Tensile strength at break point is considered as response. The operating conditions implemented are given in Table 2.

Table 2. Levels of the variables used in the experiment

Control Factors	Level					
	1	2	3	4	5	Units
Composition (code:C)	50	60	70	80	90	Weight % (HDPE)
Speed (code:S)	30	40	50	60	70	mm/min

Full-Factorial design is conducted in accordance with 5 level L_{25} (5^6) orthogonal array. The S/N ratios for maximum tensile strength at break (in MPa) under 'larger is the better characteristic' are calculated as the logarithmic transformation of the loss function as shown below.

Larger is the better characteristic:

$$\frac{S}{N} = 10 \log \frac{1}{n} \left(\sum \frac{1}{Y^2}\right) \quad (5)$$

Where 'n' is the repeated number trial conditions and 'Y' is the data pertaining to tensile strength at break point.

3. RESULTS AND DISCUSSION

3.1 Tensile, Flexural and Impact Strengths of Polyblends

In this section the mechanical strength results corresponding to 20, 30 and 50% PP reinforced composites are reported. The maximum value (≈ 35MPa) of tensile strength is resulted from PP where as the HDPE matrix bears a tensile strength of ≈ 22MPa (Fig. 3(a)). Reinforcement of PP to HDPE improves the tensile strength (compared to HDPE) due to formation of brittle polyblends as observable in Fig. 3(b). The magnitude of tensile modulus at break point is reported in Fig. 3(c). Detailed tensile results are noted in Table 6. The experimental outcomes for flexural tests are reported in Fig. 4. Flexural strength improves (See Fig. 4a) and a value of ≈ 23MPa is observed for all the composite blends. Fig. 4(b) reveals the PP added polyblends bear more extension properties when compare to HDPE. Data pertaining to the flexural modulus are reported in Fig. 4(c); indicating the PP content increases the flexural modulus; as PP to be a separate phase in the polyblend and HDPE as continuous matrix.

The impact strength of polymers are expressed in three different ways and reported in Fig. 5. The results corresponding to impact strength in Joule (J) is reported in Fig. 5(a); indicating a maximum value for HDPE where as attributing a minimum value to 50/50 polyblend. Energy absorbed during impact per unit thickness of sample is manifested in Fig. 5(b). The impact energy absorbed per unit cross sectional area, perpendicular to load; also shows a similar trend as visible in Fig. 5(c). Reinforcement of PP particles to HDPE matrices contracts the stress concentration and the plastic deformation property is lost; there by weakening the impact property.

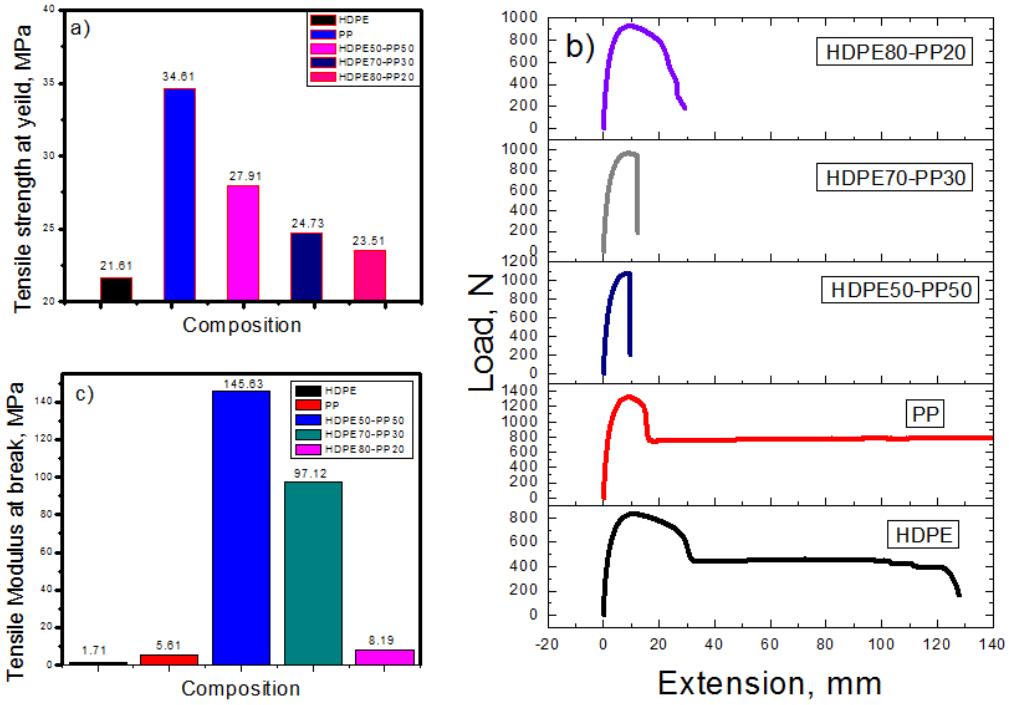

Fig. 3. Tensile properties of the polymer composites, (a) Tensile strength at yield, (b) Load against extension, (c) Tensile modulus at break

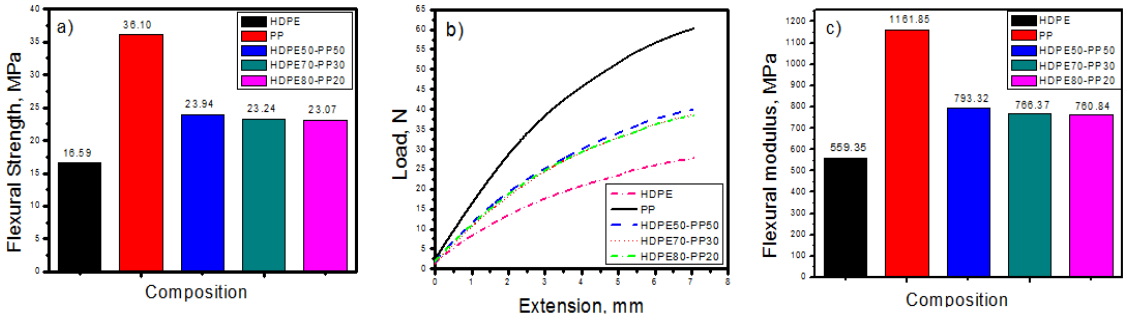

Fig. 4. Flexural properties of the polyblends, (a) Flexural strength, (b) Load vs extension, (c) Flexural modulus

3.2 Phase Analysis of HDPE/PP Polyblends

The chemical and crystal structure of HDPE/PP polyblends are analysed by XRD and FTIR. Figs. 6 and 7 reports the XRD and FTIR results. For PP all the peaks lies between 2θ of 15 to 30°, which are α form of PP. The peaks are corresponding to crystalline lattices [60]. Two diffraction peaks for HDPE are observed between 20 to 30° diffraction angles, comprising of orthorhombic crystals [61,62]. Reinforcing PP to HDPE does not produce any new peaks, only shortening of peaks for HDPE/PP polyblends are seen. So combination of PP with HDPE is only a physical mixing with no alternation of chemical structure. Table 3 shows the frequency ranges of different functional groups of PP and HDPE polymers, with assigned vibration type. The FTIR spectra reveals, the peaks of HDPE/PP composites confirms to those of virgin HDPE and PP matrices.

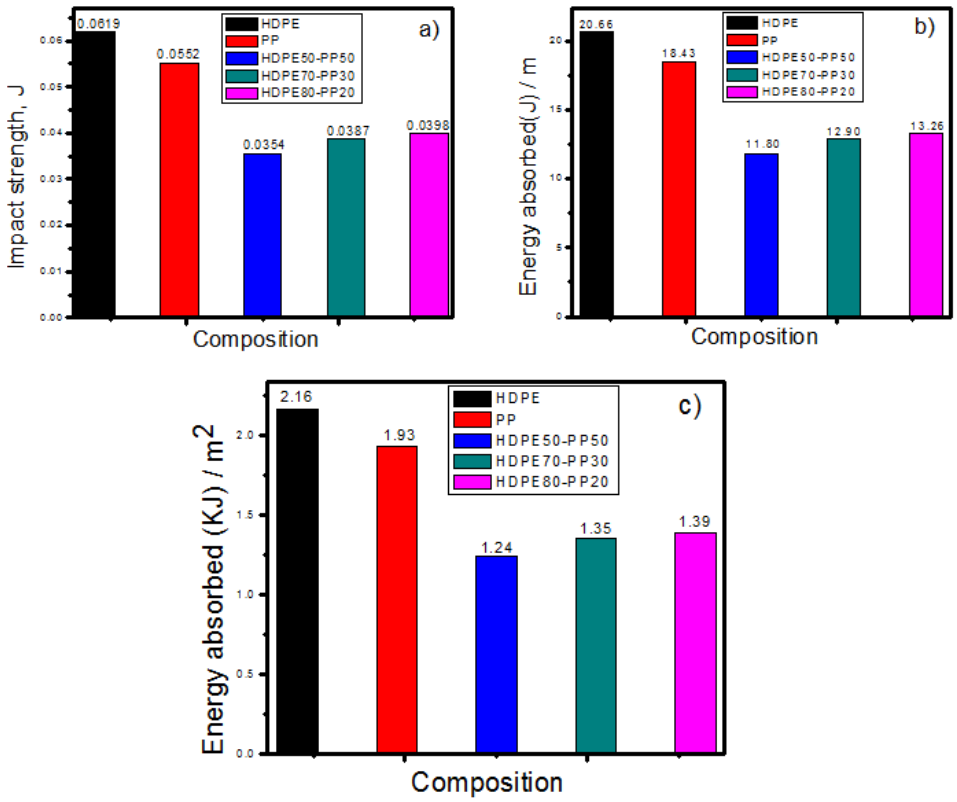

Fig. 5. Impact strengths of the polyblends, (a) Energy absorbed, (b) Energy absorbed/m of sample thickness, (c) Energy absorbed/ unit cross sectional area

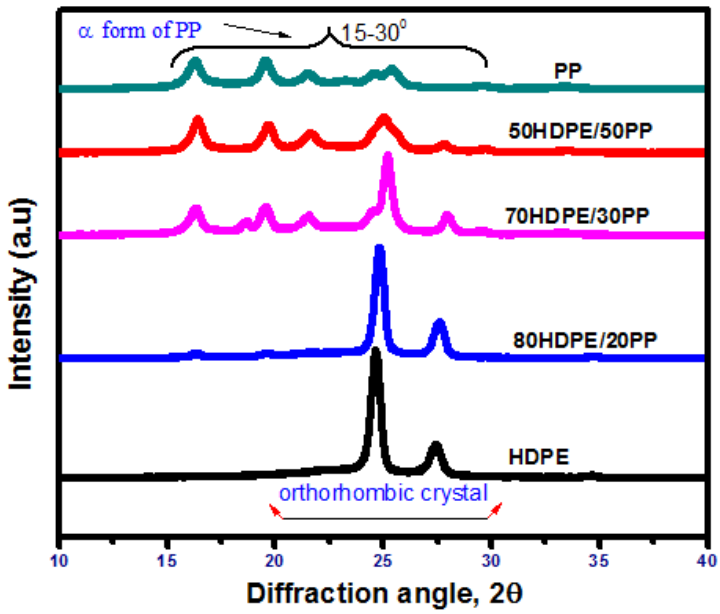

Fig. 6. X-Ray diffractogram of polymer composite blends

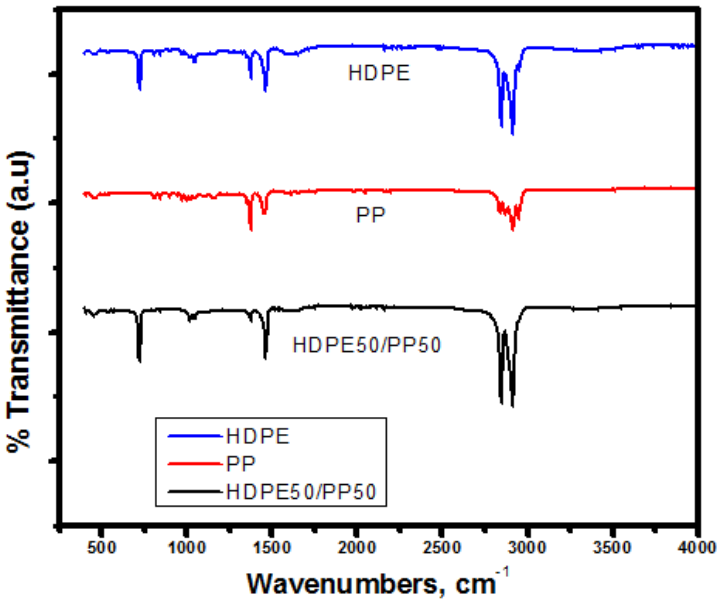

Fig. 7. FT-IR spectroscopy of polymer composite blends

Table 3. IR spectra analysis reports

Group	Wave number (cm^{-1})	Vibration type	Assigned to
-C-H	2985-2810	Stretching	PP
$-CH_2$	2950-2850	Stretching	HDPE
$-CH_2$	1475-1440	Bending	PP
$-CH_3$	1380-1370	Bending	PP
$-CH_2$	1470-1460	Bending	HDPE
$-CH_2$	730-700	Rocking	HDPE

3.3 Thermal Behaviour of HDPE/PP Polyblends

From the DSC study the melting temperature (T_m) of PP and HDPE are 168.6 and 134.6℃ respectively. Table 4 reports the detailed results of melting temperature and melt enthalpy (ΔH_f) of the polymers. The HDPE/PP polyblend bears two melt points as shown in Fig. 8(a); indicating the polyblend to be a co-occurrence of both HDPE and PP. The results authenticate the polymer composite to be a physical mixture of both the polymers. The existence of PP in HDPE does not alter the melt peak temperature significantly.

Fig. 8(b) shows the temperature (T_c) and enthalpy (ΔH_c) of crystallization for all the polymers resulted from the DSC cooling cycle. The T_c's for PP and HDPE are 122.11 and 115.01℃ respectively. Result shows PP crystallizes faster than HDPE. But the order of crystallinity of the composite blend is quite similar to HDPE. Augmentation of PP particles to HDPE retards the nucleation of the heterogeneous polymer blend and so the crystallization peaks of the polyblends are undistinguishable.

The weight loss of a polymer with respect to time or temperature is usually predicted by using TGA technique. The thermal degradation is an irreversible process. Our work focused to predict the degradation temperature (T_D). It is defined in our project as; the temperature at which the weight loss of the polymers just starts to fall immediately. Fig. 9 shows TG/DTG thermogram sketches of our prepared polymers. The results obtained via TG analysis on polymers are revealed in Table 5. All the samples undergo a single degradation step. The inflection point (I_P, at which the rate of weight change with temperature is maximum) and residual weight % are also reported in Table 5. It is evident from

the results that, the thermal behaviour of the binary polyblends differ marginally; may be due to similar density and MFI.

Table 4. DSC data of HDPE/PP polyblends

Polymer type	ΔH_f, J/g	T_m, °C	T_c, °C	X_C, %	ΔH_c, J/g
HDPE	213.9	134.6	115.0	73.0	253.2
PP	55.7	168.6	122.1	26.9	74.94
50HDPE/50PP	119.7[a]/30.5[b]	134.4[a]/166.1[b]	115.2	81.70[a]/29.46[b]	212.4
70HDPE/30PP	138.1[a]/29.6[b]	134.4[a]/163.7[b]	115.5	67.33[a]/47.66[b]	201.5
80HDPE/20PP	131.0[a]/25.1[b]	134.8[a]/162.6[b]	120.8	55.88[a]/60.62[b]	148.6

The superscript [a] and [b] corresponds to citing HDPE and PP respectively

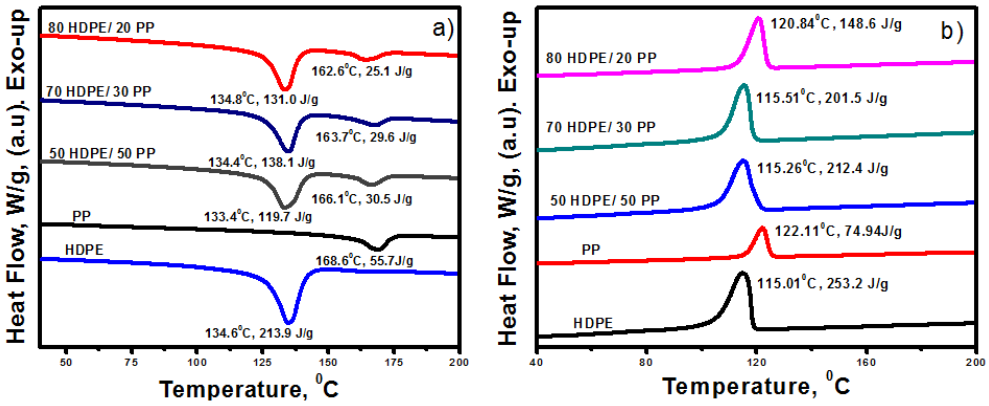

Fig. 8. DSC sketches of the obtained polyblends; (a) Heating (b) Cooling cycles

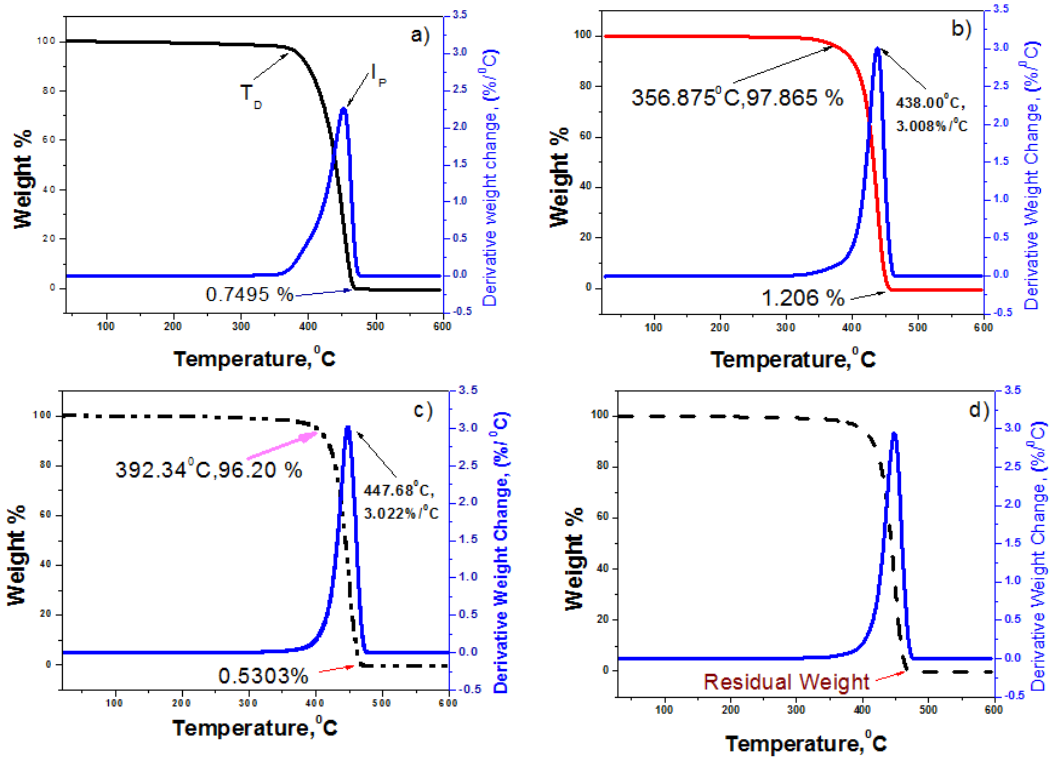

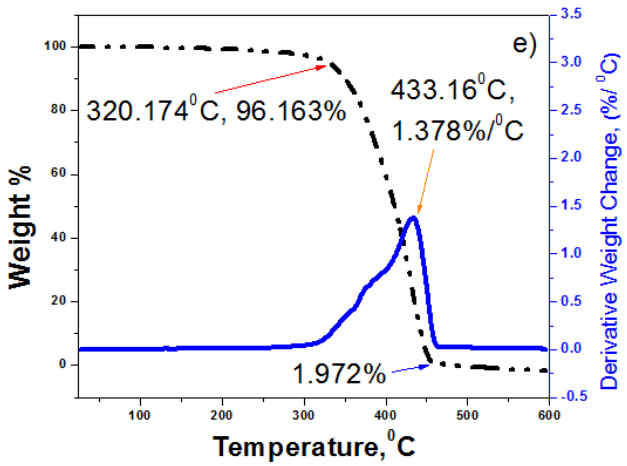

Fig. 9. TG/DTG thermograms of (a)Virgin HDPE, (b)Virgin PP, and HDPE/PP Polyblends which contain, (c) 50 wt%, (d) 30 wt% and (e) 20 wt% of PP

Table 5. TG/DTG results of prepared polymers

Sample	T_D, ℃	Weight % at T_D	Residual weight %	Inflection point	
				℃	%/℃
HDPE	368.56	97.45	0.7495	452.5	2.264
PP	356.87	97.86	1.206	438.0	3.008
50HDPE/50PP	392.34	96.20	0.5303	447.68	3.002
70HDPE/30PP	388.54	96.45	0.6602	447.65	2.94
80HDPE/20PP	320.174	96.16	1.972	433.16	1.378

3.4 Microscopy of HDPE/PP Polymer Composites

The surface morphology of polymers before fracture is reported in Fig. 10 by means of FESEM. A similar morphology of all the polymer blends is observed. Prepared sample's surfaces are smooth and difficult to differentiate by FESEM. The continuous and dispersed phases for un-fractured polyblend samples are difficult to identify. To evaluate the changes in the properties; carbon elemental mapping (EDS) and AFM tests are conducted and disclosed in Figs. 11 and 12. Surface behaviour of fractured specimens after impact test is shown in Fig. 13.

Fig. 12 reports 2D and 3D topography of the prepared tensile specimens. The polymers are uniformly distributed inside the composite as visible in the AFM images. The white and brown spots (both dark and dull) are confirming to the PP and HDPE phases respectively. Few aggregative PP phases are observed in the 50HDPE/50PP composite. A wide distribution of PP molecules within the blend is noticeable in 90 % HDPE blend (Fig. 12. (i) and Fig.12 (j)). As both the polymers are not compatible to each other, the molecular distribution of PP declines with its content. HDPE holds low melting point and high melt flow index, resulting a smoother surface formation during injection moulding. Results corresponding to the rms roughness (R_q) are revealed in Fig. 14. Attributing to the above discussion, the roughness of the prepared tensile specimen confirms to be minimum for 90HDPE/10PP polymer composite. The maximum rms roughness (R_q=3.478 nm) is resulting for 50HDPE/50PP polyblend specimen and falls with increase in HDPE load.

Crystal structures of the polyblends during solidification from molten stage are reported in Fig. 15. Spherulites are large and spherical for PP conforming to the results reported by jia-Horng Lin et al. [14], and so called ring spherulites for HDPE. PP forms an overlapped layer in the polyblend and

hence an incomplete spherulitic growth is resulting for the polymer composites. Spherulites stalk over each and cannot reach to complete form.

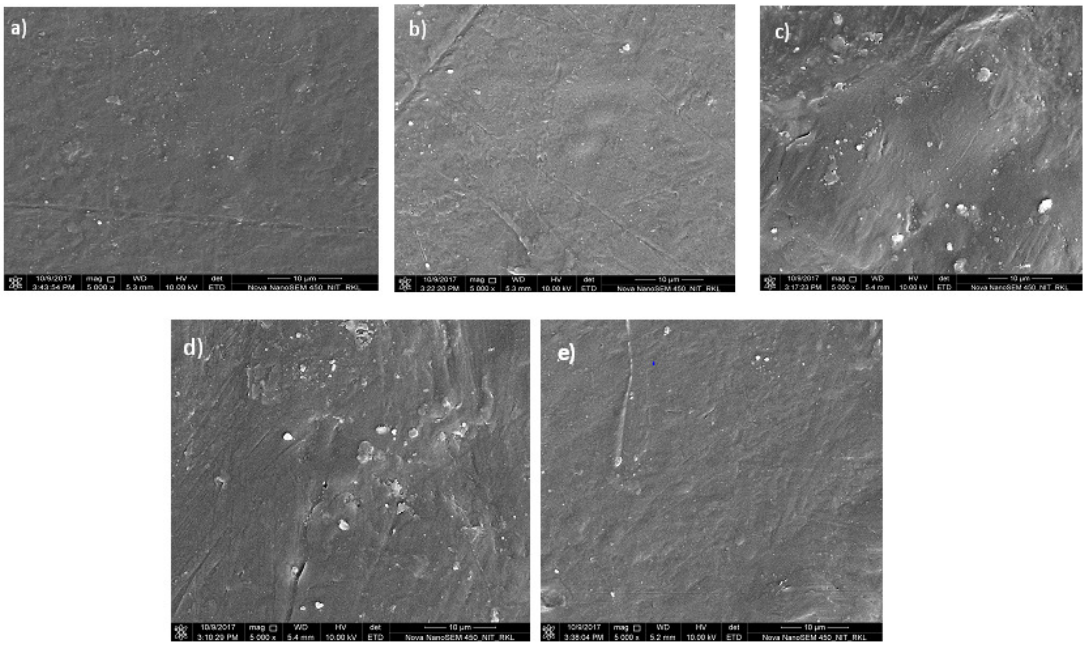

Fig. 10. Surface Morphology of un-fractured Polyblends; (a)Virgin HDPE, (b)Virgin PP, and HDPE/PP Polyblends which contain, (c) 50 wt%, (d) 30 wt% and (e) 20 wt% of PP

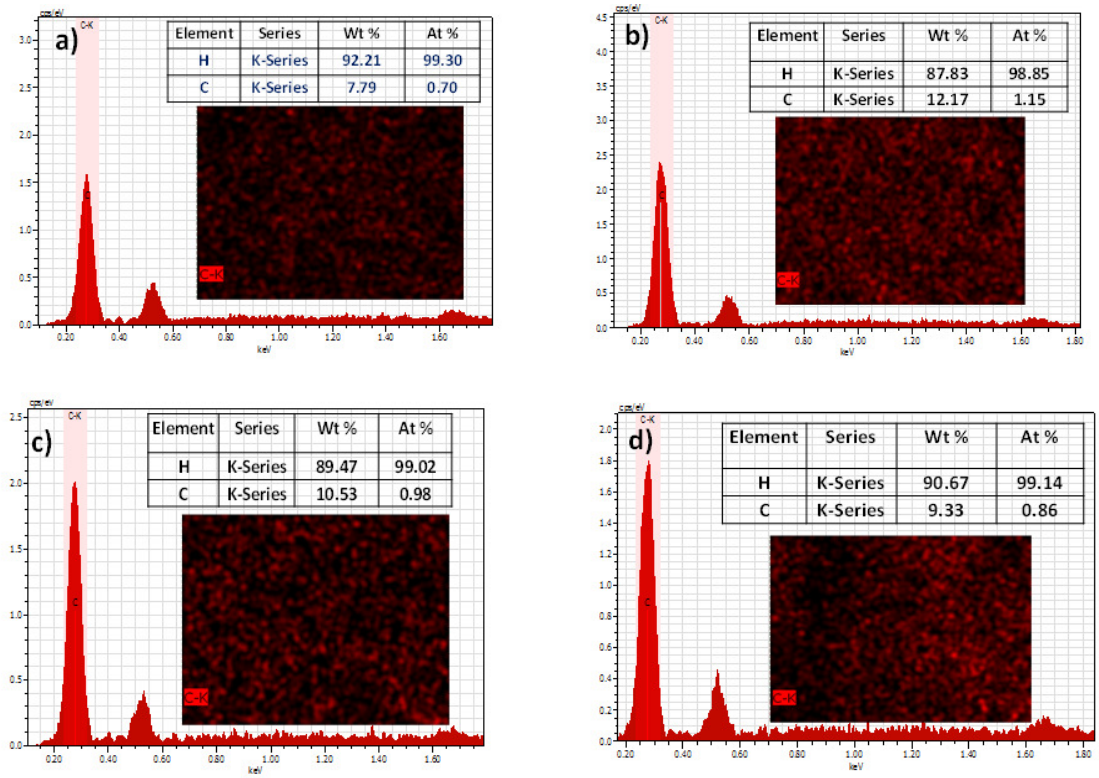

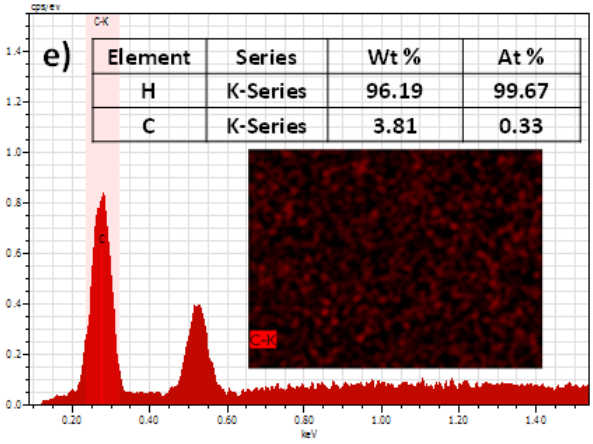

Fig. 11. EDS and Carbon element mapping of Polyblends; (a)Virgin HDPE, (b)Virgin PP, and HDPE/PP Polyblends which contain, (c) 50 wt%, (d) 30 wt% and (e) 20 wt% of PP

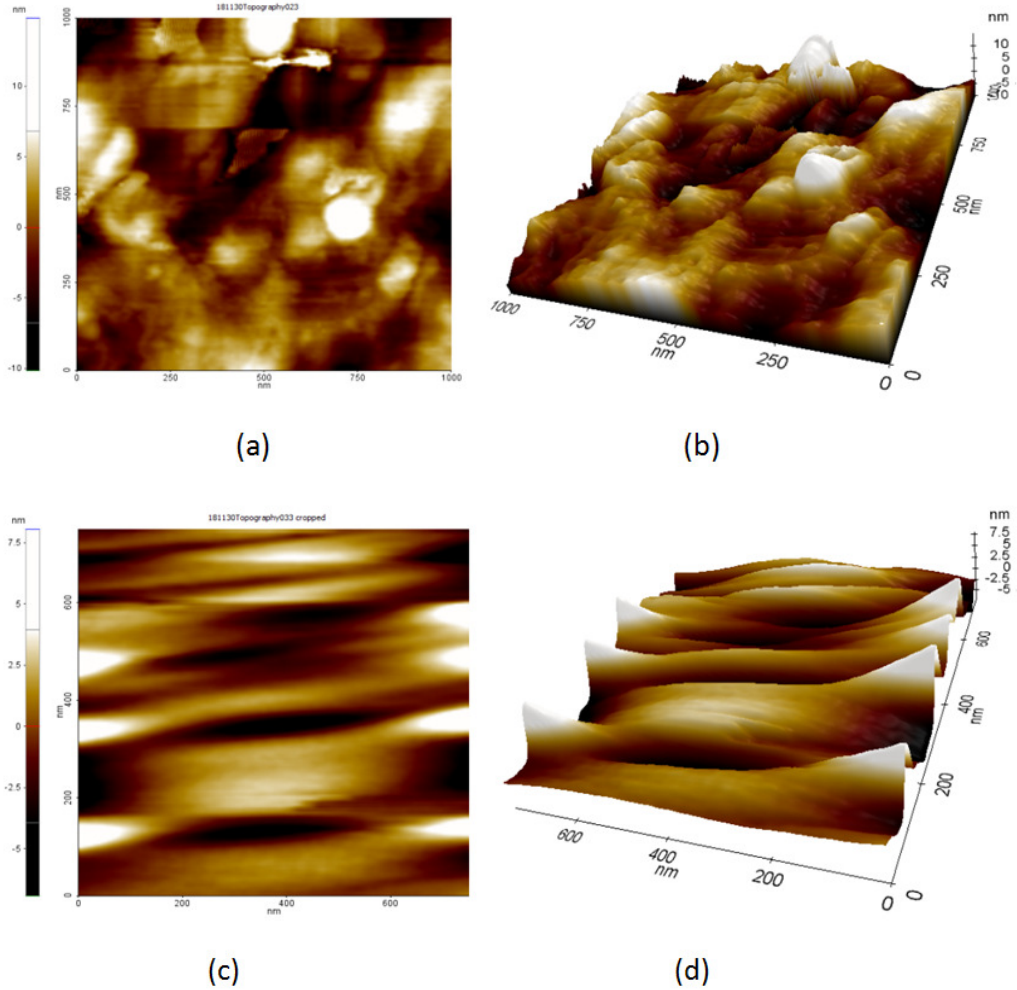

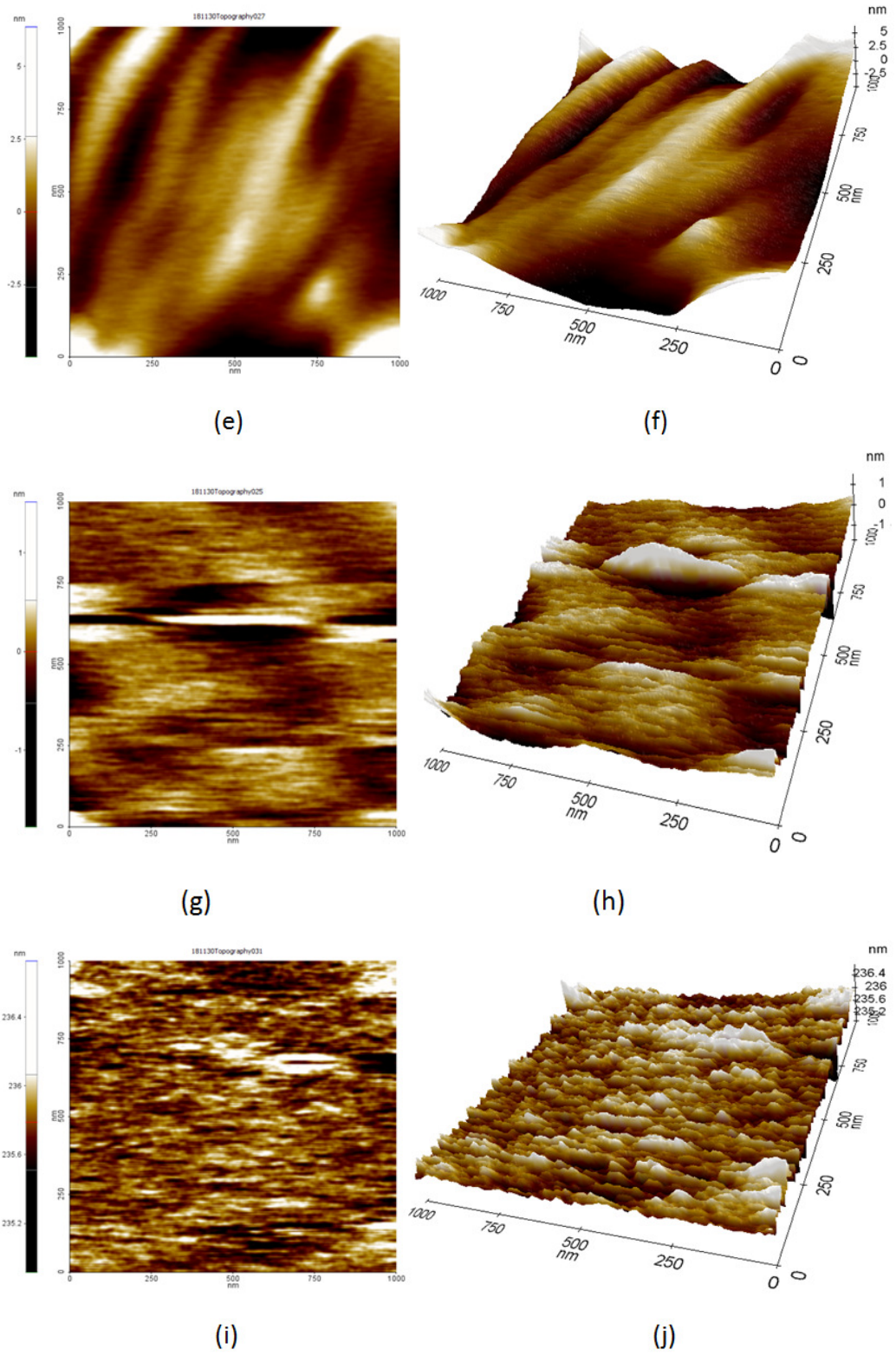

Fig. 12. 2D and 3D Tapping mode AFM images of (a),(b) 50HDPE/50PP; (c),(d) 60HDPE/40PP; (e),(f) 70HDPE/30PP; (g),(h) 80HDPE/20PP; (i),(j) 90HDPE/10PP polyblends

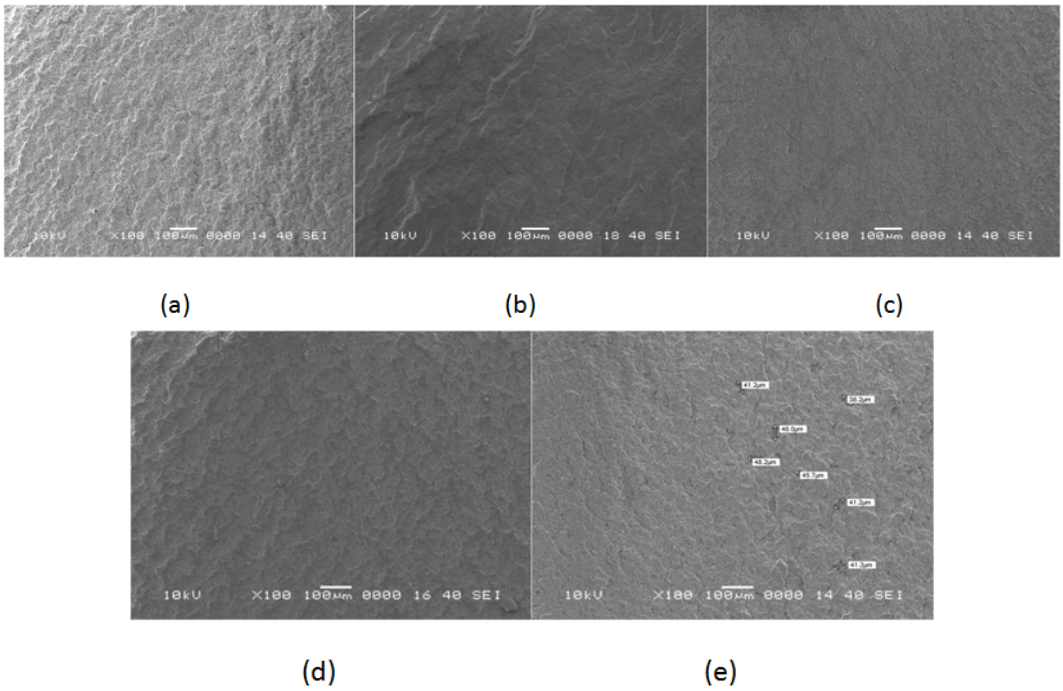

Fig. 13. SEM images of the fractured specimens after impact tests; (a) Virgin HDPE, (b) Virgin PP and Polyblends which contain (c) 50 wt %; (d) 30 wt %; (e) 20 wt % of PP

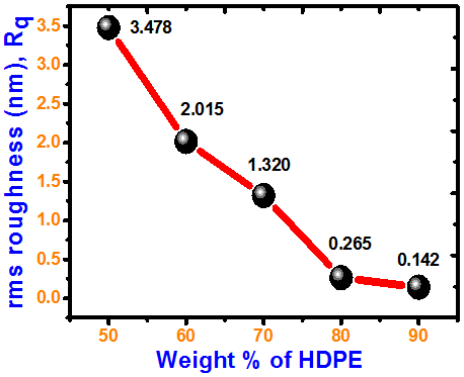

Fig. 14. Root mean square roughness (R_q) of the prepared tensile specimens

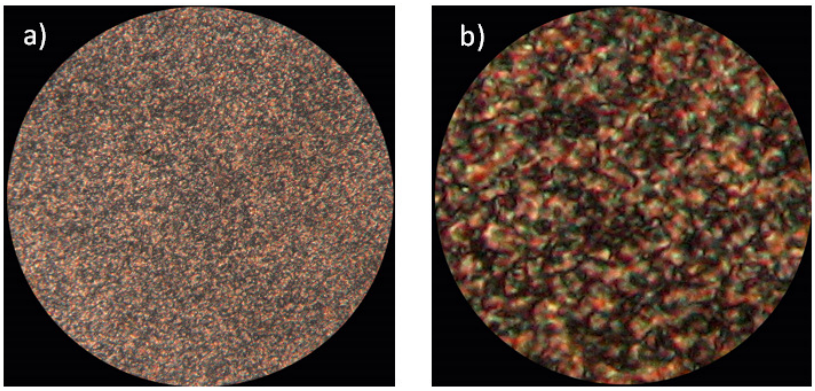

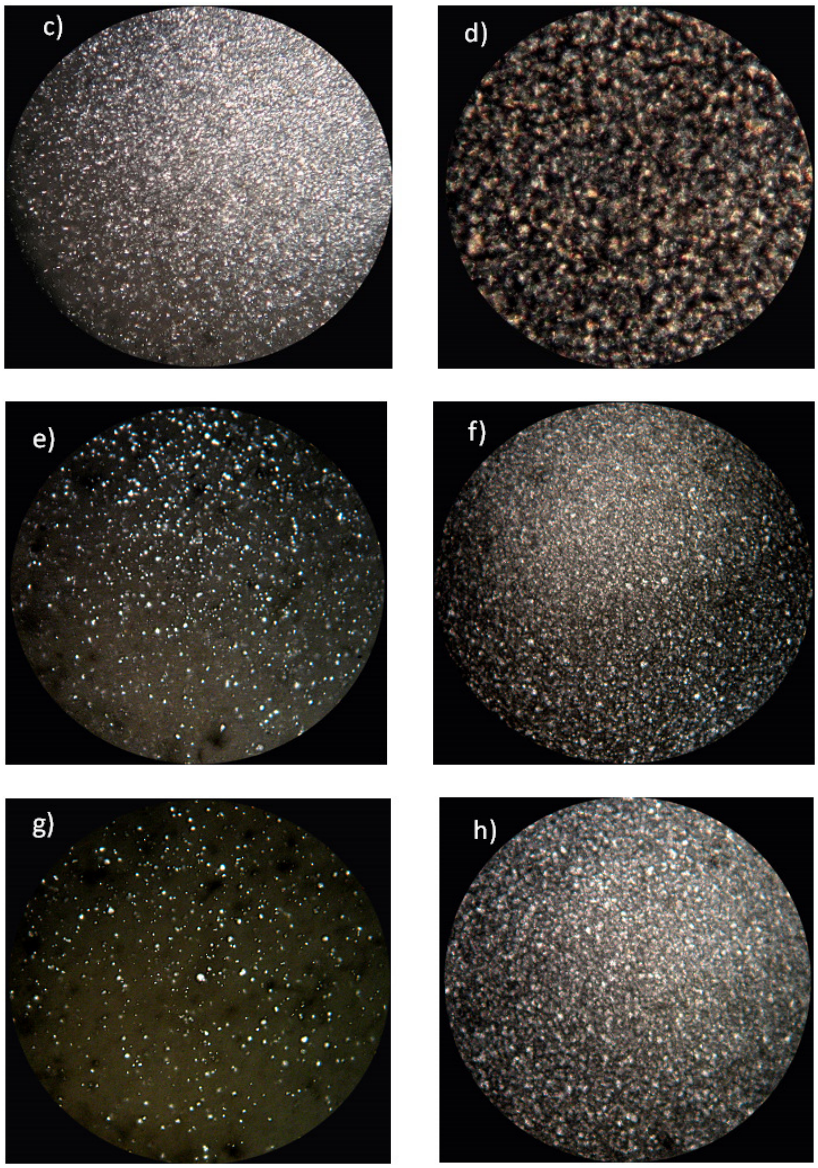

Fig. 15. Spherulite structures of prepared Polymers (a) HDPE at 130℃, (b) HDPE at 125℃, (c) PP at 130℃, (d) PP at 125℃, (e) 50HDPE/50PP at 130℃, (f) 50HDPE/50PP at 125℃, (g) 80HDPE/20PP at 130℃, (h) 80HDPE/20PP at 125℃

Electrical properties like surface resistivity and volume resistivity are measured using a super mega ohmmeter (Identification no: CIPET/PTC/095 make: Toa electronics ltd, Japan, Model: SM-8220) at a voltage of 500V as per ASTM-D 257 standard. Dielectric strength is measured using a dielectric breakdown tester (Identification No: CIPET/PTC/150, Megger, OTS 100 AF/2). Results of different electrical properties are reported in Figs. 16 to 18.

Since the surface length is fixed, the measurement of surface resistivity is independent of physical dimensions. In our observation the surface resistivity of both HDPE and PP samples are same. But the augmentation of PP with HDPE matrix increases the surface resistivity. The value is maximum for 70HDPE/30PP composite. The mechanism behind the improvement of the property is not understood in our project. Data pertaining to volume resistivity is shown in Fig. 17.

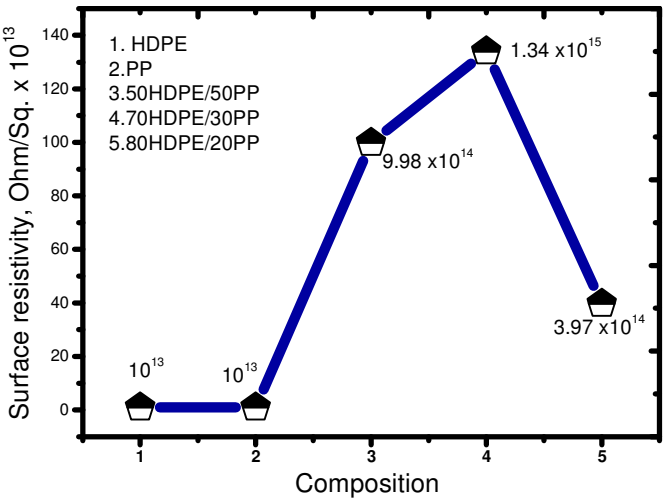

Fig. 16. Results showing data for surface resistivity

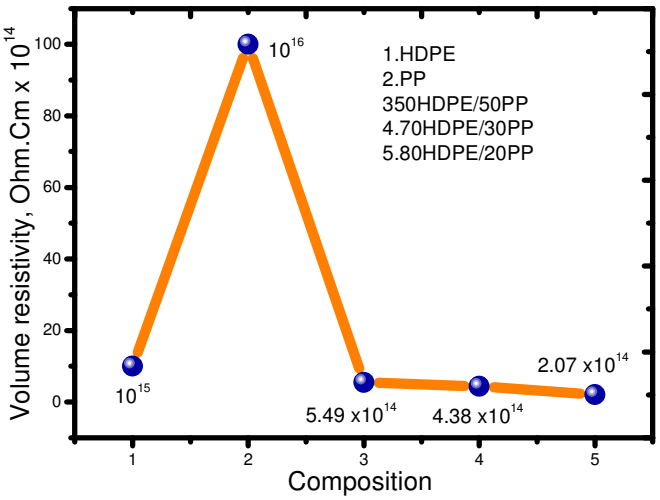

Fig. 17. Variation of Volume resistivity with composition

PP bears maximum volume resistivity of about 10^{16} ohm.cm. It is noteworthy to mention that the reinforcement of PP to HDPE matrix results in decrease of volume resistivity. The obtained results reveal, the 80HDPE/20PP composite possesses the minimum volume resistivity of 2.07 × 10^{14} ohm.cm. But the causes behind the fall in the said property are unknown.

Dielectric strength is a major electrical property of insulators. In general the electrical properties break down after continuous application of increased voltage to an insulator. So it is a measure of electrical strength of a material as an insulator. It is the maximum voltage required to produce a dielectric breakdown through the material and is expressed as volts per unit thickness. In our observation the HDPE/PP composite bears less dielectric strength than their virgin forms as shown in Figure-18. Generally the dielectric strength of a material arises due to the polarisation of molecules and it increases with increase in polarisability [63]. It is believed that the augmentation PP to HDPE matrix decreases the atomic polarisation, thereby lessening the insulating properties.

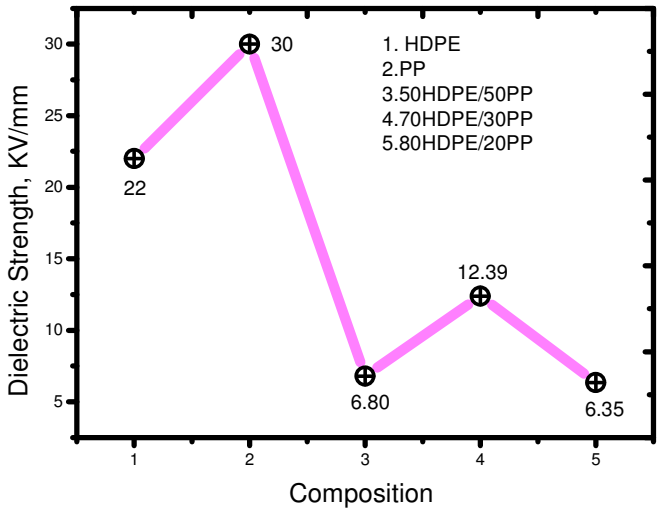

Fig. 18. Dielectric Strength as a function of composition

Table 6. Experimental values of stress at yield and break point

Composite	Speed, mm/min									
	30	40	50	60	70	30	40	50	60	70
	Stress, MPa									
	At Yield					At break				
50HDPE/50PP	27.96	25.40	27.91	26.42	27.49	25.73	23.22	26.69	25.57	26.12
60HDPE/40PP	23.74	24.53	24.85	25.60	25.78	14.39	13.07	6.26	6.85	6.44
70HDPE/30PP	25.73	26.11	24.73	27.47	27.15	23.57	24.29	24.15	25.50	25.17
80HDPE/20PP	24.20	24.60	23.51	25.15	25.65	20.63	20.40	22.10	21.79	23.99
90HDPE/10PP	27.95	28.54	29.13	29.45	29.48	2.94	3.03	5.66	5.40	7.62

Table 7. Experimental values of strain at yield and break point

Composite	Speed, mm/min									
	30	40	50	60	70	30	40	50	60	70
	Strain, %									
	At Yield					At break				
50HDPE/50PP	7.55	7.62	7.05	7.62	7.15	11.46	12.08	8.82	9.81	9.78
60HDPE/40PP	8.25	8.24	8.22	8.07	7.74	438.18	438.64	295.80	141.05	92.132
70HDPE/30PP	7.87	7.11	7.50	7.15	7.04	12.98	10.90	12.59	11.13	11.53
80HDPE/20PP	8.54	8.20	7.70	7.59	7.54	15.19	15.26	12.82	12.15	11.07
90HDPE/10PP	7.28	7.16	6.94	6.91	7.00	104.35	84.15	62.59	68.24	55.07

Finally the effect of strain rates on tensile strength of the prepared polymer composites is evaluated. Data pertaining to the tensile properties of all the prepared polyblends at different cross head speeds are reported in Tables 6 and 7. Table 6 shows the outcomes for the tensile stress at yield and break points in MPa. The resulted strain in % at both yield and break points are disclosed in Table 7.

The optimisation result shows that tensile strength is maximum for 50HDPE/50PP polyblend. The tensile strength decreases with increase in HDPE content in the composite. Tensile strength is minimum at the cross head speed of 40 mm/min and maximum at 70 mm/min. The Fig. 19 reveals, the strength is almost same at cross head speed of 40, 50 and 60 mm/min. But the improvement of the tensile strength at the rate of 70 mm/min is quite significant. Analysis of result from Figure.19 concludes that a factor combination of C1 and S5 shows the maximum strength at break point. The results are in accordance to the fact that, high strain rates favour the elastic behaviour of materials.

Elasticity is associated with load bearing performance as embodied in properties such as strength. But low strain rates favour the viscous behaviour. In our experiment; as cross head speed increases to 70 mm/min; the temperature of the specimen might declines to minimum and making it stronger and stiffer.

The tensile strength behaviour at break point is designed and reported in Table 8. S/N ratio in Taguchi's technique indicates the ranking of parameters based on their influences. The mean of the S/N ratios is found to be 22.960 dB. Response table for S/N ratios is shown in Table 9. Larger the better characteristic is taken for this analysis. The difference between the highest and lowest value estimates the magnitude of delta (Δ). Ranking was allotted in descending order with respect to the delta values. It is concluded that composition dominates in a higher extent to tensile strength; than that of cross head speed. Figs. 19 and 20 depicts the main effect plot for S/N ratio and mean S/N ratio respectively.

The analysis of variance (ANOVA) is used to analyze the influence of tensile strength parameters like composition and speed. The ANOVA establishes the relative significances of factors in terms of their percentage contribution to the response. This analysis was carried out for a level of significance of 5% (the level of confidence 95%). 'P' value, less than 0.05 for a particular parameter, indicates that it has the major effect on the responses. From Table 10 it is observed that 'P' value for the factor composition is much lesser than 0.05; so the major controlling parameter for tensile strength is composition followed by speed.

Table 8. Experimental design using L_{25} orthogonal array

L_{25} (5^6)	Composition, Wt % HDPE	Speed, Mm/min	Tensile Strength At break, MPa	S/N Ratio, dB
1	50	30	25.73	28.21183
2	50	40	23.22	27.31986
3	50	50	26.69	28.52892
4	50	60	25.57	28.15631
5	50	70	26.12	28.33946
6	60	30	14.39	23.16423
7	60	40	13.07	22.32551
8	60	50	6.26	15.93981
9	60	60	6.85	16.72015
10	60	70	6.44	16.18581
11	70	30	23.57	27.44977
12	70	40	24.29	27.70927
13	70	50	24.15	27.65942
14	70	60	25.50	28.13217
15	70	70	25.17	28.01973
16	80	30	20.63	26.29251
17	80	40	20.40	26.19431
18	80	50	22.10	26.88824
19	80	60	21.79	26.76634
20	80	70	23.99	27.6006
21	90	30	2.94	9.378756
22	90	40	3.03	9.654614
23	90	50	5.66	15.0686
24	90	60	5.40	14.6527
25	90	70	7.62	17.64594

A correlation between tensile strength at break point "TS_b" (non-variable factor), composition and speed (variable factors) is derived by multiple linear regressions from equation no-6. From equation no-4, it is observed that the factor "composition" has a major impact on tensile strength followed by speed.

Table 9. Response table for tensile strength at break

Level	Composition: C	Speed: S
1	28.11	22.9
2	18.87	22.64
3	27.79	22.82
4	26.75	22.89
5	13.28	23.56
Delta(Δ)	14.83	0.92
Rank	1	2

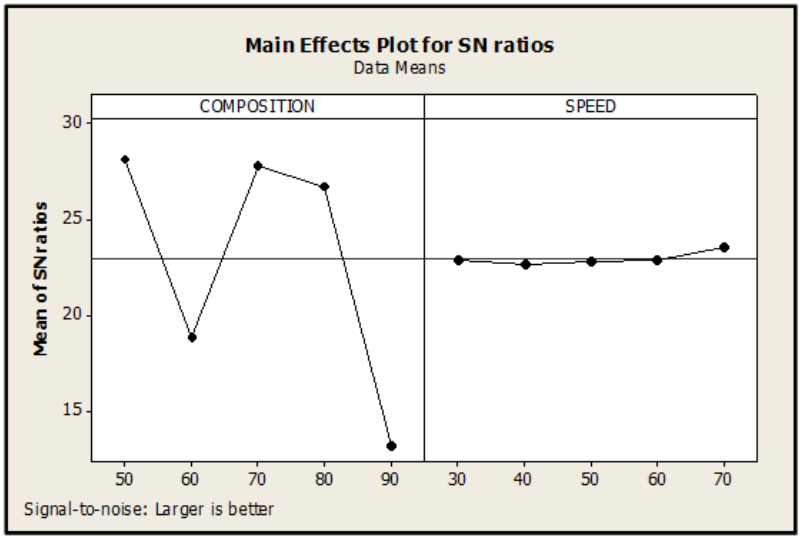

Fig. 19. Main effect plot for S/N ratio

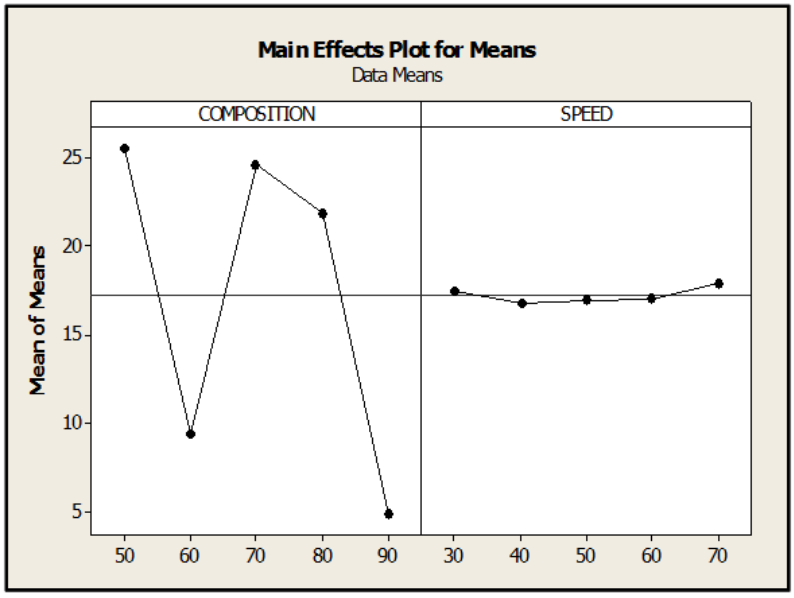

Fig. 20. Main effect plot for means

Table 10. ANOVA table for tensile strength at break point

Source	DF	Seq SS	Adj SS	Adj MS	F	P
COMPOSITION	4	873.54	873.54	218.38	33.83	0
SPEED	4	2.45	2.45	0.61	0.09	0.983
Error	16	103.29	103.29	6.46		
Total	24	979.28				

NOTE - DF: Degree of Freedom; seq SS: The Sequential Sum of Squares; Adj SS: Adjusted Sum of Squares; Adj MS: Adjusted Mean Squares

$$TS_b = K_0 + K_1A + K_2B + K_3C \quad (6)$$

Where, K_i (i = 0, 1, 2, 3….) is a model constant. The regression equation is given by

$$TS_b = 36.8 - 0.287\ COMPOSITION + 0.010\ SPEED \quad (7)$$

Finally a confirmation test was conducted to evaluate the design parameters influencing the response. The purpose of confirmation experiment is to validate the conclusions drawn during the analysis phase. For this, control parameters with optimal levels of 60HDPE/40PP for composition and 40 mm/min for speed are considered. Table 11 shows the confirmation test result. The experimental result shows an improvement in tensile strength at break point to be 1.6%.

Table 11. Results of the confirmation experiment

	Optimal control parameters	
	Prediction	**Experimental**
Level	C_2S_2	C_2S_2
S/N ratio, dB	22.85	23.22

4. CONCLUSION

Our project promisingly combines PP with HDPE. The dispersion of PP in HDPE improves tensile and flexural strengths compared to HDPE, where as impact strength falls in compared to both HDPE and PP. The XRD, FTIR and DSC tests prove the polyblend to be a combination of two dispersed matrices. No changes in chemical structure are observed, confirming the composite to be a physical blending. PLM tests authenticate; reinforcement of PP particles to HDPE retards the crystal growth and spherulites lap over. The spherulite growth rate is higher for virgin PP than HDPE. TGA tests disclose the degradation characteristics. The polyblend shows lesser values of dielectric strength and volume resistivity. On the other hand the surface resistivity is improved. The exact causes for the changes in the property are not clear. But it is believed may be due to changes in the polarising property. Cross head speed is an important variable to decide the tensile behaviour. Tensile strengths at break point are quite identical at 40, 50 and 60 mm/min and the value is maximum at 70 mm/min. Optimisation results summarises composition is more dominating to tensile strength compared to cross head speed. The results are quite obvious due to the stated reasons. Surface roughness of the tensile specimens is significantly affected by the presence of PP; as dispersed phase in the composite. The polyblend having 50 weight % of PP and HDPE holds the highest rms roughness during moulding. Due to low material cost and traditional fabrication methods, the polymer composites may find suitable applications areas.

COMPETING INTERESTS

Authors have declared that no competing interests exist.

REFERENCES

1. Erbetta CDC, Azevedo RCS, Andrade KS, eSilva MESR, Roberto FS. Characterization and lifetime estimation of high density polyethylene containing a prodegradant agent. Materials Sciences and Applications. 2017;8(13):979-991.

2. Bertin S, Robin J. Study and characterization of virgin and recycled LDPE/PP blends. European Polymer Journal. 2002;38:2255–2264.
3. Laoutid F, Estrada E, Michell RM, Bonnaud L, Müller AJ, Dubois P. The influence of nanosilica on the nucleation, crystallization and tensile properties of PP–PC and PP-PA blends. Polymer. 2013;54:3982–3993.
4. Xie BH, Huang X, Zhang GJ. High thermal conductive polyvinyl alcohol composites with hexagonal boron nitride microplatelets as fillers. Composites Science and Technology. 2013;85: 98–103.
5. Ma W, Zhang J, Wang X. Crystallizaion and surface morphology of poly (vinylidene fluoride)/poly (methylmethacrylate) films by solution casting on different substrates. Applied Surface Science. 2008;254:2947–2954.
6. Albano C, González J, Ichazo M, Rosales C, Urbina de Navarro C, Parra C. Mechanical and morphological behavior of polyolefin blends in the presence of $CaCO_3$. Composite Structures. 2000;48:49–58.
7. Hsieh CT, Pan YJ, Lin JH. Polypropylene/high-density polyethylene/carbon fiber composites: Manufacturing techniques, mechanical properties, and electromagnetic interference shielding effectiveness. Fibers and Polymers. 2017;18(1):155-161.
8. Wilkinson AN, Laugel L, Clemens ML, Harding VM, Marin M. Phase structure in polypropylene/PA6/SEBS blends. Polymer. 1999;40:4971–4975.
9. Tseng FP, Lin JJ, Tseng CR. Poly (oxypropylene)-amide grafted polypropylene as novel compatibilizer for PP and PA6 blends. Polymer. 2001;42:713–725.
10. Shi H, Shi D, Wang X, Yin L, Yin J, Mai YW. A facile route for preparing stable co-continuous morphology of LLDPE/PA6 blends with low PA6 content. Polymer. 2010;51:4958–4968.
11. Maciel A, Salas V, Manero O. PP/EVA blends: Mechanical properties and morphology. Effect of compatibilizers on the impact behavior. Advances in Polymer Technology. 2005;24:241–252.
12. Martins CG, Larocca NM, Paul DR, Pessan LA. Nanocomposites formed from polypropylene/EVA blends. Polymer. 2009;50:1743–1754.
13. Valera-Zaragoza M, Rivas. Influence of morphology on the dynamic mechanical characteristics of PP-EP/EVA/organoclay nanocomposites. Composites Part B: Engineering. 2013;55:506–512.
14. Lin JH, Pan YJ, Liu CF, Huang CL, Hsieh CT, Chen CK, Lin ZY, Lou CW. Preparation and compatibility evaluation of polypropylene/high density polyethylene polyblends. Materials. 2015;8:8850–8859.
15. Souza AMC, Demarquette NR. Influence of composition on the linear viscoelastic behavior and morphology of PP/HDPE blends. Polymer. 2002;43:1313–1321.
16. Li J, Shanks RA, Long Y. Mechanical properties and morphology of polyethylene–polypropylene blends with controlled thermal history. Journal of Applied Polymer Science. 2000;76:1151–1164.
17. Jose S, Aprem AS, Francis B, Chandy MC, Werner P, Alstaedt V, Thomas S. Phase morphology, crystallisation behaviour and mechanical properties of isotactic polypropylene/high density polyethylene blends. European Polymer Journal. 2004;40:2105–2115.
18. Macosko CW, Jeon HK, Hoye TR. Reactions at polymer–polymer interfaces for blend compatibilization. Progress in Polymer Science. 2005;30:939–947.
19. Saroop M, Mathur GN. Studies on the dynamically vulcanized polypropylene (PP)/butadiene styrene block copolymer (SBS) blends: Mechanical properties. Journal of Applied Polymer Science. 1997;65:2691–2701.
20. Van Puyvelde P, Velankar S, Moldenaers P. Rheology and morphology of compatibilized polymer blends. Current Opinion in Colloid and Interface Science. 2001;6:457–463.
21. Camacho W, Karlsson S. NIR, DSC and FTIR as quantitative methods for compositional analysis of blends of polymers obtained from recycled mixed plastic waste. Polymer Engineering Science. 2001;41:1626–1635.
22. Teroda M, Ohaba Y. Energy transfer mechanism and amplified spontaneous emission characteristics of dye mixture solutions. Journal of Applied Physics. 1983;22:1392.

23. Gulrez SKH, Ali Mohsin ME, Shaikh H, Anis A, Pulose AM, Yadav MK, Qua EHP, Al-Zahrani SM. A review on electrically conductive poly-propylene and polyethylene. Polymer Composites. 2014;35:900-914.
24. Walker BM, Rader CP, (Eds.). Handbook of thermoplastic elastomers. Van Nostrand Reinhold, New York; 1979.
25. Malik TM, Prud'hornme RE. Dielectric properties of Poly(α-Methyl α-n-Propyl-β-Propiolactone)/Poly(Vinyl Chloride) blends. Polymer Engineering and Science. 1984;24(2):144.
26. Pathrnanathan K, Cavaille JY, Johari GP. Dielectric relaxations of microstructurally different latex polymer blends of Poly(Butyl Acrylate) and Poly(Vinyl Acetate)Polymer. 1988;29:311.
27. Maistros GM, Block H, Bucknall CB, Patridge IK. Dielectric monitoring of phase separation during cure of blends of epoxy resin with carboxyl-terminated Poly (Butadiene-Co-Acrylonitrile). Polymer. 1992;33(21):4470.
28. Pillai PKC, Narula GR, Tripathy AK. Dielectric properties of Polypropyl-ene/Polycarbonate polyblends. Polymer Journal. 1984;16(7):575.
29. Radhakrishnan S, Saini DR. Structure and dielectric properties of Poly(Vinyl Chloride) thermoplastic elastomer blends. Journal of Applied Polymer Science. 1994;52:1577.
30. Gustafsson A, Salot R, Gedde UW. Electrical degradation of blends and laminar composites of polyethylene and polystyrene. Polymer Composites. 1993;14:5421.
31. Mansour AA, Sabagh SEL, Yehia AA. Dielectric investigation of SBR-NBR and CR-NBR blends. Journal Elastomers and Plastics. 1994;26:367.
32. Elashmawi IS, Hakeem NA, Abdelrazek EM. Spectroscopic and thermal studies of PS/PVAc blends. Physica B: Condensed Matter. 2008;403:3547.
33. Ramesh S, Yahaya AH, Arof AK. Miscibility studies of PVC blends (PVC/PMMA and PVC/PEO) based polymer electrolytes. Solid State Ionics. 2002;148:483.
34. Rawat A, Mahavar HK, Tanwar A, Singh PJ. Study of electrical properties of Polyvinylpyrrolidone/Polyacrylamide blend thin films. Bulletin of Materials Science. 2014;37:273-279.
35. Mothé C, Monteiro D, Mothé M. Dynamic mechanical and thermal behavior analysis of composites based on polypropylene recycled with vegetal leaves. Materials Sciences and Applications. 2016;7:349-357.
36. Pillai PKC, Gupta AK, Goel M. Study of surface potential characteristics of corona charged ethyl cellulose layers for its relevance in electrothermography. Macromolecular Chemistry. 1980;181: 951.
37. Krishnakumar B, Gupta RK, Forster EO, Laghari JR. The effect of polypropylene morphology on AC breakdown. Annual Report Conference on Electrical Insulation and Dielectric Phenomena. 1986;522.
38. Wagner H. The influence of superstructures on the electrical breakdown of partially crystalline polymers. Annual Report Conference on Electrical Insulation and Dielectric Phenomena. 1974;62.
39. Kawahigashi M, Miyashita Y, Kato H. Chemical structures of copolymers and their electrical properties. Rec. IEEJ EIM Study Meeting, EIM-89-50. 1989;39. (In Japanese)
40. Yamakita T. Morphology and dielectric breakdown of blend polymers. Rec. IEEJ EIM Study Meeting, EIM-90-77. 1990;1. (In Japanese)
41. Katsunami K, Ishii K, Tanaka Y, Ohki Y. Dielectric properties of polymer blend of polypropylene and polyethylene. Proceedings of the 3rd International Conference on Properties and Applications of Dielectric Materials July 8-12, Tokyo, Japan; 1991.
42. Favaro S, Pereira A, Fernandes J, Baron O, da Silva C, Moisés M, Radovanovic E. Outstanding impact resistance of post-consumer HDPE/Multilayer packaging composites. Materials Sciences and Applications. 2017;8(1):15-25.
43. Erbetta CDC, Azevedo RCS, Andrade KS, eSilva MESR, Roberto FS. Characterization and lifetime estimation of high density polyethylene containing a prodegradant agent. Materials Sciences and Applications. 2017;8(13):979-991.

44. Mendes L, Cestari S. Printability of HDPE/Natural fiber composites with high content of cellulosic industrial waste. Materials Sciences and Applications. 2011;2(9):1331-1339.
45. Jacob GC, Starbuck JM, Feller JF, Simunovic S, Boeman RG. Strain rate effects on the mechanical properties of polymer composite materials. Journal of Applied Polymer Science. 2004;94:296–301.
46. Salih S, Hamood A, Alsalam A. Comparison of the characteristics of LDPE: PP and HDPE: PP polymer blends. Modern Applied Science. 2013;7(3):33-42.
47. Sahoo PC, Murmu R, Patra SC, Dutta C, Sutar H. Electrical behaviour and spherulites morphology of HDPE/PP polyblends with HDPE as base material. Materials Sciences and Applications. 2018;9:837-843.
48. Sutar H, Sahoo PC, Sahu PS, Sahoo S, Murmu R, Swain S, Mishra SC. Mechanical, thermal and crystallization properties of Polypropylene (PP) reinforced composites with High Density Polyethylene (HDPE) as matrix. Materials Sciences and Applications. 2018;9:502-515.
49. Sutar H, Maharana H, Dutta C, Murmu R, Patra S. Strain rate effects on tensile properties of HDPE-PP composite prepared by extrusion and injection moulding method. Materials Sciences and Applications. 2019;10:205-215.
50. Omar MF, Jaya H, Akil HM, Ahmad ZA, Noriman NZ. Mechanical properties of High Density Polyethylene (HDPE)/sawdust composites under wide range of strain rate. Applied Mechanics and Materials. 2015;754-755:83-88.
51. Abdel-Hakim AA, Abdel-Salam Sabbah I, Metwally MS, El Begawy S, Elshafie ES. Mechanical properties and morphology studies of nanocomposites based on RSF/Nanoclay modified /HDPE nanocomposites. Life Science Journal. 2012;9(3):134-142.
52. Rahman MR, Islam MN, Huque MM, Hamdan S, Ahmed AS. Effect of chemical treatment on Rice Husk (RH) Reinforced Polyethylene (PE) composites. BioResources. 2010;5(2):854-869.
53. Yang HS, Kim HJ, Son J, Park HJ, Lee BJ, Hwang TS. Rice-husk flour filled polypropylene composites; mechanical and morphological study. Composite Structures. 2004;63(3):305-312.
54. Bai SL, Cao K, Chen JK, Liu ZD. Tensile properties of rigid glass bead/HDPE composites. Polymers and Polymer Composites. 2000;8(6):413-418.
55. Reis JML, Pacheco LJ, da Costa Mattos HS. Influence of the temperature and strain rate on the tensile behavior of post-consumer recycled high-density polyethylene. Polymer Testing. 2013;32:1576–1581.
56. Siviour CR, Jordan JL. High strain rate mechanics of polymers: A review. Journal of Dynamics Behaviour of Materials. 2016;2:15–32.
57. Dhoble A, Kulshreshtha B, Ramaswami S, Zumbrunnen DA. Mechanical properties of PP-LDPE blends with novel morphologies produced with a continuous chaotic advection blender. Polymer. 2005;46:2244-2256.
58. AlMaadeed MA, Labidi S, Krupa I, Ouederni M. Effect of waste wax and chain structure on the mechanical and physical properties of polyethylene. Arabian Journal of Chemistry. 2015;8:388–399.
59. Blaine RL. Thermal Applications Note. Polymer Heats of Fusion.
60. Nishino T, Matsumoto T, Nakamae K. Surface structure of isotactic polypropylene by X-ray diffraction. Polymer Engineering and Science. 2000;40:336–343.
61. Inci B, Wagener KB. Decreasing the alkyl branch frequency in precision polyethylene: Pushing the limits toward longer run lengths. Journal of American Chemical Society. 2011;133:11872–11875.
62. Liao CZ, Tjong SC. Mechanical and thermal performance of high-density polyethylene/alumina nanocomposites. Journal of Macromolecular Science. Part B. 2012;52:812–825.
63. Ku CC, Leiens R. Eleclrical properties of polymers: Chemical principles. Hanser Publishers, Munich-Vienna, New York; 1987.

Biography of author(s)

Harekrushna Sutar
Department of Chemical Engineering, Indira Gandhi Institute of Technology, Sarang, India.

He is working as an assistant professor in Indira Gandhi Institute of Technology, Sarang, Odisha, India. He has obtained BE (Utkal University, Bhubaneswar) and ME (Jadavpur University, Kolkata) in chemical engineering. He has obtained PhD (Engineering) at Jadavpur University in the field of Plasma spray coating technology. He has worked as Technical Assistant at National Institute of Technology, Rourkela for one year. He has 3 years research experience at Bhabha Atomic Research Centre, Bombay. He is working in the research areas of coating technology, tribology, polymer science, composite materials, water treatment, fluidization and bioremediation. He has published about 30 peer reviewed research papers in national and international journals. He is editorial board member of Journal of Engineering Research and Reports (JERR) and Chemical Science International Journal (CSIJ). He has supervised several undergraduate projects and five post graduate project till date. He is life member of professional bodies like Institution of Engineers (India), Indian Institute of Chemical Engineer, IACSIT (Singapore), IAENG (USA). Mr Sutar is a potential reviewer of several ISI and non-ISI Journals. His Google Scholar ID is 5aT1HesAAAAJ, Publons ID is 1219719. In this book chapter he has designed the study, wrote the protocol and wrote the first draft of the manuscript.

Rabiranjan Murmu
Department of Chemical Engineering, Indira Gandhi Institute of Technology, Sarang, India.

He is working as an assistant professor at Indira Gandhi Institute of Technology, Sarang, Odisha, India for the last five years. He is graduated in chemical engineering from Biju Patnaik University of Technology, Rourkela with first class. Thereafter he obtained M.Tech degree in chemical engineering from Indian Institute of Technology, Madras. He is engaged in teaching the subjects like Chemical Reaction Engineering, Heat Transfer, Chemical Engineering Thermodynamics, Chemical Process Technology and Numerical Methods. His research interest includes Proton conducting Membrane for Fuel Cell, Biodiesel Production, Modeling and Simulation of fuel cell stack, Semiconducting Materials, thin film and surface coating. He possesses the software skills like MATLAB, Aspen plus, Origin lab, MS Office, MINI TAB etc. He has published around 10 research papers in international journals of repute. His Google Scholar ID is NqZ6oVgAAAAJ. In reference to this book chapter, he has conducted the experimental data analysis and revision.

Chiranjit Dutta
Department of Chemical Engineering, Indira Gandhi Institute of Technology, Sarang, India.

He is a chemical engineer. He is graduated from Indira Gandhi Institute of Technology, Sarang, India in the year 2018. He has qualified GATE in the year 2018 and pursuing M.Tech in chemical engineering with process control and instrumentation as

specialisation at National Institute of Technology, Trichy, India. He has two journal papers to his credit. He has worked on the study of drying kinetics of food particles using fluidized bed dryer as his undergraduate project. In reference to this book chapter he has done literature review.

Mutlu Ozcan
Head of Division of Dental Biomaterials Center for Dental and Oral Medicine Clinic for Fixed and Removable Prosthodontics and Dental Materials Science, University of Zurich, Switzerland.

She has earned her Dentistry Licenciate in 1993 in Istanbul, Turkey, Dr. med. dent. degree in 1999 in Cologne, Germany and Doctorate in Medical Sciences (PhD) in 2003 in Groningen, The Netherlands. She received full professorship for Clinical Dental Biomaterials at the University of Groningen, The Netherlands in 2007. Since 2009, she is the Director of Division of Dental Biomaterials at the University of Zurich, Switzerland. She also holds Honorary Professorship positions at various universities some of which are São Paolo State University (Brazil), University of Florida (USA), and University of Hong Kong (China). She has authored more than 500 ISI Web of Science indexed original scientific and clinical publications, is a well-sought lecturer, receiver of several international awards, and serves for the editorial boards of numerous scientific journals. She is European Prosthodontic Association (EPA)-recognized Specialist in Prosthodontics, Honorary Secretary of the EPA, Immediate Past-President of the International Association of Dental Research (IADR)/Dental Materials Group (DMG), Fellow of Academy of Dental Materials (FADM), Fellow of International College of Dentistry (FICD), and Fellow in Dental Surgery of the Royal College of Physicians and Surgeons of Glasgow, FDS RCPS (Glasgow). She is the recipient of the “2018 IADR Distinguished Scientist Wilmer Souder Award”. Her clinical expertise is on reconstructive dentistry and her scientific work focuses on translational research. With respect to this book chapter she has suggested experimental ideas for successfully completing the project.

Subash Chandra Mishra
Department of Metallurgical and Materials Engineering, National Institute of Technology, Rourkela, India.

He is working as full time professor in Metallurgical and Materials Engineering department at National Institute of Technology, Rourkela. He has obtained PhD in Materials Science from IIT Kharagpur. His broad research area includes Thermal Plasma an HVOF Coatings, Plasma and Reactive Plasma Processing of Materials, Processing and Characterizations of Industrial Waste and Bio-waste reinforced Polymer Composites, Utilization of Bio-wastes/bio-mass for Production of Activated Carbon and Bio-Char. He has successfully completed 11 funded projects from different agencies like DST, MHRD, CSIR, DAE, UGC, Nalco, and Tata Steel. He has about 20 books, 1 book chapter, 2 patents, 200 refereed journal papers, 100 conference proceedings to his credit. He is nominated as AICTE expert for southern zone, northern zone of India. He is life Member of IIM (I), IE (I), IIME. He has produced 7 PhD scholars and 6 PhD scholars are continuing under him. He has supervised more than 50 M.Tech project. He has received several national and international awards. He was the Commonwealth Fellow (Visiting Fellow, University of Liverpool). He was awarded as “Leading Scientist of the World”, by International Biographical centre, Cambridge, England (in the arena of metallurgical and materials engineering) in 2010. His Google Scholar ID is tMT8UIgAAAAJ. Concerning to the present book chapter, he has supervised the work and given the work plan.